Journal of Pharmaceutical Analysis 14 (2024) 284–286

Contents lists available at ScienceDirect

Journal of Pharmaceutical Analysis

journal homepage: www.elsevier.com/locate/jpa

Short communication

Enhanced identification and localization of metabolites in Scutellariae Radix using ion mobility enabled MALDI-Q-TOF/MS imaging

Lixing Nie [a], Lieyan Huang [b], Xiaofei Jia [c], Shuai Kang [a], Lingwen Yao [a], Yanpei Wu [a], Hao Yuan [d], Yongli Liu [d], Feng Wei [a], Hongyu Jin [a, *], Xiang Li [e, **], Shuangcheng Ma [a, ***]

[a] National Institutes for Food and Drug Control, Beijing, 102629, China
[b] Chinese Academy of Medical Science and Peking Union Medical College, Beijing, 100006, China
[c] Waters Corporation, Beijing, 102600, China
[d] Hebei Institute for Drug and Medical Device Control, Shijiazhuang, 050227, China
[e] Department of Pharmacy, Medical Supplies Center of the PLA General Hospital, Beijing, 100853, China

ARTICLE INFO

Article history:
Received 30 June 2023
Received in revised form
21 September 2023
Accepted 28 September 2023
Available online 4 October 2023

Unraveling the distribution of metabolites in traditional Chinese medicine (TCM) provides direct indications for understanding their regulatory and functional basis, which is of paramount significance for better utilization and quality control of medicinal plants [1]. Recently, imaging techniques such as near-infrared spectroscopy, Raman spectroscopy, and mass spectrometry (MS) were explored to reveal the spatial context of component accumulation and localization [2,3]. Among them, matrix-assisted laser desorption ionization combined with quadrupole time-of-flight MS (MALDI-Q-TOF/MS) is the most prevalent technology for mass spectrometry imaging (MSI) of natural products in tissue sections [4]. Though possessing high spatial resolution, the identification of the constituents of TCM is difficult because of interference from the matrix, especially for small molecules. MALDI MSI coupled with ion mobility (IM) has been successfully employed for the separation of matrix/background and endogenous components in animal and human tissues [5]. However, its application in plant tissues, such as in TCM, has scarcely been reported. This Short communication describes the first adoption of IM-enabled MALDI MSI of metabolites in TCM. By determining both the ion *m*/*z* and IM drift time, endogenous metabolites from the cross section of the Scutellariae Radix could be clearly distinguished from interference from the matrix. Hence, small deviations in the mobility drift times were observed for six different molecular species. In particular, flavonoids exhibited a distinct spatial distribution trend line in two-dimensional (2D) contour map of the mobility-*m*/*z* data, allowing for the identification of their specific molecular type. Distinct ion distribution images were eventually obtained for baicalin and the other components. The combination of IM with MALDI MSI improved the selectivity and efficiency of chemical profiling, providing new perspectives for the visualization of phytochemicals in TCM.

Scutellariae Radix samples were collected from Chengde, China. Rootlets and soil were removed from the surface, and the roots were dried under the sun. Their origins were authenticated by Dr. Shuai Kang, and specimens were preserved in National Institutes for Food and Drug Control. The middle part of the root was cut into 30-μm cross sections before thaw-mounted on indium tin oxide-coated (ITO) glass slides. Two slices were prepared for each sample. Twenty layers of 2-nitrophloroglucinol (NPG) solution were sprayed as the matrix. To optimize instrument parameters and facilitate identification, MALDI-MS, MALDI-MS/MS, mobility-enabled MALDI-MS, and mobility-enabled MALDI-MS/MS analyses were performed on reference standards and sample tissues using a SYNAPT XS HDMS traveling wave IM Q-TOF mass spectrometer with a MALDI interface. MS data were acquired in positive ion mode from *m*/*z* 100 to 1,200. MS images were acquired at a spatial resolution of 30 μm with 600 laser shots per position. The collision energies were 2 V in MS mode and 20–60 V for different daughter ions in MS/MS mode. Phosphorus red at 10 mg/mL prepared in acetone was used for calibration and lockmass to acquire high-resolution mass spectra. The assignments of the detected ions were based on the exact masses and on-tissue tandem mass data, with reference to the MS and MS/MS data of the standards as well as databases and literature. For further confirmation of the assignment results, ultrahigh performance liquid chromatography (UHPLC) coupled with an Orbitrap Fusion Lumos Tribrid mass

Peer review under responsibility of Xi'an Jiaotong University.
* Corresponding author.
** Corresponding author.
*** Corresponding author.
E-mail addresses: jhyu@nifdc.org.cn (H. Jin), lxyjylk@163.com (X. Li), masc@nifdc.org.cn (S. Ma).

https://doi.org/10.1016/j.jpha.2023.09.018

spectrometer was employed for the analysis of Scutellariae Radix extract. All MALDI-MS data were processed and analyzed using HDImaging™ (v1.5) software. MS images were displayed in absolute intensity after total ion current normalization. IM data were processed by DriftScope (v2.9) software. The recognition of raw mass data obtained by UHPLC-Orbitrap Fusion Lumos Tribrid/MS, alignment, and matching of the peaks were performed on Compound Discoverer (v 3.1).

Flavonoid reference standards were analyzed by MALDI-MS, MALDI-MS/MS, MALDI-IM-MS, and MALDI-IM-MS/MS to optimize the experimental methods for the detection of these compounds in tissues. After IM separation, the precursor ion corresponding to each flavonoid was selected for MS/MS fragmentation. Using baicalin as an example, Fig. S1 shows the background noise reduction ability of the IM spectrometry. The extracted arrival time distribution was used to select fragment ions produced only from the reference standards. Compared with the MALDI-MS/MS spectrum extracted from the ion chromatogram (Fig. S1A), the MALDI-IM-MS/MS spectrum was much "cleaner" (Fig. S1B), enabling a more selective detection and identification of the components.

The mass spectra of Scutellariae Radix, both with and without mobility separation, exhibited similar mass peaks. Two cross sections were analyzed, and they yielded identical identification and distribution results. Although the distribution patterns differed slightly, the mobility drift times of the identified metabolites in the different samples were identical. A slight reduction in intensity was observed in the mobility-enabled MALDI spectra. The inclusion of an IM separation step in the analysis did not affect the sensitivity of the method or increase the acquisition time. Using tandem mass analysis of the slices and UHPLC-Orbitrap Fusion Lumos Tribrid/MS confirmation, six different classes of metabolites, including 26 flavonoids, two saccharides, one phenylpropanoid, one coumarin, one anthraquinone, and one alkaloid, were identified by direct tissue analysis. The chemical name, CAS No., chemical class, formula, adduct ion, theoretical *m*/*z*, observed *m*/*z*, mass accuracy, fragments, and mobility drift time of detected compounds were listed in Table S1. To reveal the background noise, an equivalent area of the NPG matrix on ITO glass without root tissue was also scanned. The *m*/*z* values of the detected ions were all below 500, indicating that interference from the matrix originated primarily from small molecules. Fig. 1 shows a MALDI-IM-TOF/MS 2D contour plot of the mobility drift time of the ions versus their *m*/*z* values. The dots corresponding to the assigned components of the root tissue and background noise were clearly distinguishable. The gray blocks on the top were ions ascribed to the matrix, whereas the bottom dots with other colors corresponded to endogenous metabolites of Scutellariae Radix, whose mobility was consistently lower than that of the background noise. Mobility resolutions between 17 and 40 could be used to separate endogenous metabolites from matrix interference. Furthermore, small deviations in the mobility drift time were observed within the endogenous molecules. A trend line covering all the detected flavonoids was added to Fig. 1 to provide visual guidance. Compared to flavonoids (yellow dots), compounds from other chemical classes, such as coumarins (green dots), saccharides (blue dots), anthraquinones (purple dots), phenylpropanoids (orange dots), and alkaloids (red dots), were distributed farther from the trend line. It was proven that metabolites could be separated into chemical categories in the mobility drift cell based on their differences in collision cross-sections. A closer look at the scatter plot of flavonoids indicated that the $[M+H]^+$ ion of baicalein, $[M+Na]^+$ ion of baicalein, $[M+H]^+$ ion of baicalin, and $[M+Na]^+$ ion of baicalin were distributed almost in a straight line, implying that IM could aid the assignment of the same component in the form of different adduct ions and facilitate the identification of flavones and their glycosides. Overall, the aforementioned results demonstrate the potential of mobility-enabled MALDI-MS as a powerful approach for MS imaging of TCM. This technique has the potential to mitigate the need for more complicated techniques (e.g., MS/MS) to determine the presence of molecules in tissue. Nevertheless, different drift times corresponding to the same *m*/*z* values were not observed in this case. It is difficult to distinguish between isomers that share the same molecular formula and fragmentation patterns. The combination of derivatization or cyclic IM with MSI will be attempted in the next step to resolve the flavonoid isomers detected in this study.

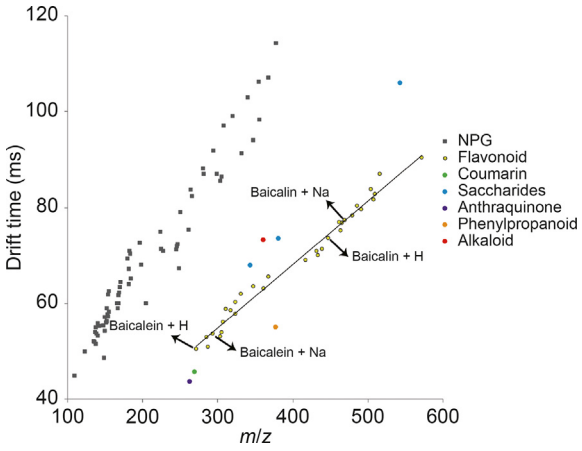

Fig. 1. Ion mobility (IM)-mass spectrometry (MS) two-dimensional (2D) plot of the endogenous metabolite ions of flavonoids (yellow dots), coumarin (green dot), saccharides (blue dots), anthraquinone (purple dot), phenylpropanoid (orange dot), and alkaloid (red dot) in the root section of Scutellariae Radix and the background ions in the matrix (gray blocks). A black trend line covering all the detected flavonoids was added to guide the eye. NPG: 2-nitrophloroglucinol.

The optimized MALDI-IM-MS approach was used to identify and localize metabolites in the cross-section of Scutellariae Radix. Optical (Fig. 2A) and MS images of the typical metabolites in the tissue are shown in Fig. 2. As shown in Figs. 2B and C, although variations in ion intensity were observed, baicalein and wogonin shared a similar spatial distribution throughout the root section, including a relatively preferential occurrence on the outer side of the cambium. As for the corresponding glycosides, baicalin and wogonoside were widely localized throughout the tissue, whereas wogonoside showed slight enrichment in the xylem of the root (Figs. 2D and E). Notably, the predominant localization of wogonoside was also found in wood rays (Figs. 2E and F, with a narrowed color gradation), indicating the transportation of this component through the conduit. Regarding saccharides, intense signals of sucrose and raffinose were detected throughout the root section, with preferential localization in the cambium (Figs. 2G and H). MALDI-IM-MS can produce images with less interference from background ions, ensuring that the biologically relevant distribution of an ion of interest is being observed and providing more precise localization than MALDI MSI alone.

MALDI-MS and MALDI-IM-MS were used to examine the distribution of the metabolites in Scutellariae Radix. Mobility-enabled MALDI-Q-TOF/MS produced 2D contour plots of IM time versus *m*/*z*, demonstrating its additional utility in separating endogenous molecules from matrix interference. The corresponding trend line for flavonoids helped differentiate them from other phytochemicals. Including an IM separation step in the MALDI MSI experiment enhanced the confidence of the identification results, allowing distinct localization of endogenous metabolites from the tissue and reducing interference from background ions.

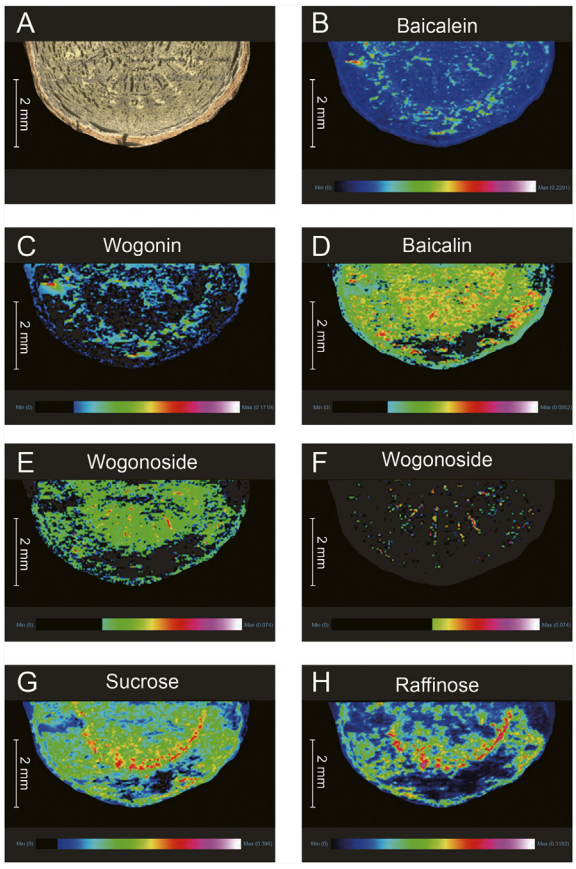

Fig. 2. (A) Optical image of Scutellariae Radix and (B–H) the matrix assisted laser desorption ionization (MALDI)-ion mobility (IM)-mass spectrometry (MS) images of the ions of baicalein (B), wogonin (C), baicalin (D), wogonoside with normal color gradation (E) and narrowed color gradation (F), sucrose (G), and raffinose (H). For each ion, a color scale from white, pink, red, yellow, green, and blue to blank indicates a descending absence of the signals.

CRediT author statement

Lixing Nie: Conceptualization, Investigation, Writing - Original draft preparation; **Lieyan Huang:** Investigation, Data curation, Visualization, Validation; **Xiaofei Jia:** Software; **Shuai Kang** and **Lingwen Yao:** Resources; **Yanpei Wu:** Software; **Hao Yuan**, **Yongli Liu**, **Feng Wei**, and **Hongyu Jin:** Resources; **Xiang Li:** Writing - Reviewing and Editing; **Shuangcheng Ma:** Supervision.

Declaration of competing interest

The authors declare that there are no conflicts of interest.

Acknowledgments

This work was supported by the National Natural Science Foundation of China (Grant No.: 81773874).

Appendix A. Supplementary data

Supplementary data to this article can be found online at https://doi.org/10.1016/j.jpha.2023.09.018.

References

[1] J. Feng, H. Ren, Q. Gou, et al., Comparative analysis of the major constituents in three related polygonaceous medicinal plants using pressurized liquid extraction and HPLC-ESI/MS, Anal. Methods 8 (2016) 1557–1564.
[2] C. Xie, W. Zhou, A review of recent advances for the detection of biological, chemical, and physical hazards in foodstuffs using spectral imaging techniques, Foods 12 (2023), 2266.
[3] J. Hou, Z. Zhang, W. Wu, et al., Mass spectrometry imaging: New eyes on natural products for drug research and development, Acta Pharmacol. Sin. 43 (2022) 3096–3111.
[4] C. Sun, L. Cui, B. Zhou, et al., Visualizing the spatial distribution and alteration of metabolites in continuously cropped *Salvia miltiorrhiza* Bge using MALDI-MSI, J. Pharm. Anal. 12 (2022) 719–724.
[5] E.K. Sisley, J. Ujma, M. Palmer, et al., LESA cyclic ion mobility mass spectrometry of intact proteins from thin tissue sections, Anal. Chem. 92 (2020) 6321–6326.